CHAPTER 2

CHAPTER 2

Theoretical Approaches on the Synergistic Interaction between Double-Headed Anionic Amino Acid Based Surfactants and Hexadecyltrimethylammonium Bromide

ABSTRACT

Theoretical investigations on the micellization of mixtures of 1) amino acids based anionic surfactants [(C_{12}AAS)Na_2: *N*-dodecyl derivatives of aminomalonate, -aspartate and -glutamate] and 2) hexadecyltrimethylammonium bromide (HTAB), were carried out at different mole ratios. Variation in the theoretical values of critical micelle concentration (*CMC*), mole fraction of surfactants in the micellar phase (X), at the interface (X^{σ}), interaction parameters at the bulk/interface (β^{R}/β^{σ}), ideality/non-ideality of the mixing processes, and activity coefficients (f) were evaluated using Rubingh, Rosen, Motomora, and Sarmoria-Puvvada-Blankschtein (SPB) models. *CMC* values significantly deviate from the theroretically calculated values, indicating associative interaction. With increasing mole fraction of (C_{12}AAS)Na_2 ($\alpha_{(C_{12}AAS)_2M_2}$), the magnitude of the (β^{R}/β^{σ}) values gradually decreased, considered to attributable to hydrophobic interactions. With increasing $\alpha_{(C_{12}AAS)_2Na_2}$, the micellar mole fraction of HTAB (X_2) decreased insignificantly and X_2 values were higher than those compared to (C_{12}AAS)Na_2 for all combinations, due to the dominance of HTAB in micelles. Micellar mole fraction at the ideal state of (C_{12}AAS)Na_2 (X_1^{ideal}) differed from micellar mole fraction of (C_{12}AAS)Na_2 (X_1), indicating non-ideality in the mixed micellization process. Gibbs free energy of micellization (ΔG_m) values are more negative than the free energy of micellization for ideal mixing (ΔG_m^{ideal}), indicating the micellization process is spontaneous. With increasing $\alpha_{(C_{12}AAS)_2Na_2}$ the enthalpy of micellization (ΔH_m) and entropy of micellization (ΔS_m) values gradually increased, which indicates micellization is exothermic. The different physicochemical parameters of the mixed micelles are correlated with the variation in the spacer length between the two carboxylate groups of (C_{12}AAS)Na_2.

J. Surfact. Deterg. (2020) 23, 891-902
DOI: 10.1002/jsde.12412

1. INTRODUCTION

Synergistic interaction between two oppositely charged surfactants in aqueous medium mainly depends on the composition, and environmental parameters such as temperature, pressure, salinity and solvent type are of secondary importance.[2-5] They also exhibit significantly lower critical micellar concentration (*CMC*) compared to the surfactants in neat form. Hydrophobic interactions and non systematic interfacial packing also result in lower *CMC*.[159] Studies of mixed surfactants include cationic/anionic,[86] cationic/cationic,[160] cationic/non-ionic,[161] anionic/non-ionic,[162] and zwitterionic/anionic,[163] systems, among others. Many mixed surfactant systems exhibit synergistic interactions, resulting in a *CMC* that is considerably lower than the *CMC* of the constituent surfactants, suitable for applications. [194]

The present work describes a theoretical investigation on the mixing behavior, synergistic interaction and structural parameters in the molecular level for the mixed micelles of three synthesized dicarboxylic amino acid based surfactants (C_{12}AAS)Na_2: *N*-dodecyl derivatives of amino-malonate,-aspartate and -glutamate in combination with hexadecyltrimethylammonium bromide (HTAB). We have investigated the interfacial and micellar aggregation behavior using different experimental techniques, such as, conductivity, surface tension, ultraviolet-visible (UV-vis) absorption/emission spectroscopy and dynamic light scattering (DLS), to determine different physicochemical parameters, *viz*., surface excess (Γ_{max}), minimum molecular area at air-water interface (A_{min}), surface pressure at the *CMC* (π_{CMC}), change in the standard free energy of micellization (ΔG^0_{mic}), Gibbs free energy of interfacial adsorption (ΔG^0_{ads}), and aggregation number (n).[85,195] As a continuation of the earlier works, well established theoretical formalisms were used to describe the micellization behavior of structurally heterogeneous surfactant mixtures.[157] However the formalisms are not predictive; as the experimentally fitted empirical interaction parameter values are mixture dependent. Previously determined experimental *CMC* values for the pure as well as mixed systems of (C_{12}AAS)Na_2 and HTAB were used and subsequently analyzed using different

computerized models in assessing the micellar composition and associated interaction parameters between the surfactants, herein used as mixed surfactant systems. Clint's phase separation model relates the mole fraction and *CMC* of mixed components in case of ideal mixing.[119] Rubingh et al.[196] established a theoretical model on the basis of regular solution theory (RST); this theory predicts the interaction between the constituent surfactants.[1] Extended the Rubingh model from bulk phase behavior to the monolayer at the air-water interface. Motomura et al. (1984) proposed the mixed micellar model based on ideal consideration, which implies that there occur no interactions (either attractive or repulsive, between the surfactant components. Sarmoria et al. (1992) have proposed mixed micelle formation involving a surfactant based phase separation model.[197] Developed a molecular thermodynamics theory in developing the binary and ternary mixed surfactant systems. In the present work, all the aforementioned formalisms were taken into account in analyzing the different structural and compositional parameters of mixed micelles of different combinations.[198]

In order to shed further light in this field of research, the present work endeavors to study the synergistic interaction between the oppositely charged mixed surfactant systems.[44, 179] HTAB-(C_{12}AAS)Na_2 mixed systems are highly relevant in terms of their wide range of applications in industries, *viz.*, enhanced oil recovery,[185] wastewater treatment,[14] textile wetting,[15] detergency,[16] paper manufacturing,[199] pharmaceutical production,[200] fabrication of nanostructured materials,[181] drug delivery,[182] cell lysis,[183] microemulsion formulation,[184] molecular separation,[185] lubrication,[186] cleaning operations,[201] and antimicrobial activity.[202] (C_{12}AAS)Na_2, capable of forming vesicles, shows manifold applications in biochemical research,[22] foaming control, surfactant-based separation,[23] surface wetting modification and flotation.[24] The two carboxylate groups of (C_{12}AAS)Na_2 do not interact prominently with HTAB, because during hydration, polar head groups of (C_{12}AAS)Na_2 associate with water molecules. Hence, (C_{12}AAS)Na_2 alone are not suitable as individual surfactants for the formation of micelles. Because *CMC* values of (C_{12}AAS)Na_2 are relatively high, it is quite rational to combine (C_{12}AAS)Na_2 with HTAB, to achieve a lower *CMC*.

The main aim of this work is to investigate on the structure and composition of mixed micelles in the molecular level using different proposed models, *viz.,* Clint, Rubingh, Rosen, Motomura and Sarmoria-Puvvada-Blankschtein (SPB). Method of iteration was adopted towards these endeavors. Different thermodynamic parameters of all the three combinations were evaluated from the theoretically calculated and experimentally determined *CMC* values using computation. It is believed that studies on the micellar structure and composition of surfactant mixtures can provide new insights, which will eventually help in understanding its bulk and interfacial properties that would also minimize the experimental circumscription.

2. EXPERIMENTAL SECTION

2.1. Materials. Hexadecyltrimethylammonium bromide (HTAB) was purchased from Sigma-Aldrich Chemicals Pvt. Ltd (St. Louis MO, USA). Lauroyl chloride, L-aspartic acid and L-glutamic acid were the products from Acros Organics Pvt. Ltd (Mumbai, India). Aminomalonic acid diethyl ester hydrochloride was purchased from TCI Pvt. Ltd (Tokyo, Japan). Hydrochloric acid, pyridine and sodium hydroxide were purchased from VWR (Stockholm, Sweden).

2.2. Synthesis of the (C_{12}AAS)Na_2 (amino acid based surfactants): Synthesis of (C_{12}AAS)Na_2 were described in literature.[25, 124]

2.2.1. Synthesis of sodium N- dodecyl amino aspartate and glutamate: A suspension of amino acid (310 mmol) was prepared in a mixture of water/acetone (210 mL /150 mL) mixture in a round-bottom flask. pH was controled at 12 with an automatic titrator filled with a solution of sodium hydroxide at 2.5 M. Lauroyl chloride was added dropwise under constant staring at 278K and stirring was continued for 90 min. The mixture was then cooled to 273K and pH was set at 12 and stirred for 2 h. The solution was warmed at 295K and acidified at pH = 2. The white precipitate was then filtered and washed with water. The product was crystallized three times from the toluene. The product was dissolved in ethanol and a solution of sodium hydroxide (2M) was added, leading to precipitate which was isolated by filtration. The final yields of $C_{12}AspNa_2$ and $C_{12}GluNa_2$ were 74 and 76 % respectively.

2.2.2. Synthesis of sodium N- dodecyl aminomalonate: The diethyl ester of the amino acid (47 mmol) was dissolved in pyridine (100 mL) in a round-bottom flask. Lauroyl chloride (47 mmol) in THF (100 mL) was added under stirring at room temperature. The suspension was stirred for 18 h and was then poured in 1.5 L (1M) hydrochloric acid. After 2 h stirring the solid diethyl ester of dicarboxylate surfactant was filtered, washed with water and dissolved in ethanol (150 mL). Sodium hydroxide (2 M, 2 eqv.) in ethanol (30 mL) was then added, leading to a white precipitate, which was isolated by filtration. The final purity of $C_{12}MalNa_2$ was 76%. All the surfactants were found to be more than 98% pure after recrystallization.

3.2. Instrumentation.

3.2.1. Surface tension studies. Surface tension was recorded by a du Noüy tensiometer with an accuracy of 0.1 mNm^{-1} (Jencon, Kolkata, India). From the break point of the surface tension *vs. log*C (surfactant concentration) plot, *CMC* was determined. [85, 203]

3.2.2. Conductance studies. Conductance values were recorded by a direct reading conductivity meter, Con 510 (Eutech Instruments, Singapore) with an accuracy of ± 0.1 μS cm^{-1}. From the break point of the conductance *vs.* [C] plots, *CMC* values were determined. [88]

3.2.3. UV-vis absorbance and emission spectroscopic studies. UV-vis absorption spectra were obtained by a spectrophotometer (UVD-2950, Labomed Inc., LA, California, USA). The sum of the absorbance of pyrene (A_T) was plotted against [C]. From the midpoint of the sigmoidal plot, *CMC* value was calculated.[48] Fluorescence spectroscopic measurements were performed by a spectrofluorometer (Hitachi High Technologies Fluorescence Spectrophotometer Corporation, F-7100, Tokyo, Japan), where *CMC* was also obtained from the sigmoidal curve, in the I_1/I_3 *vs.* [C] plot, where I_1 is the first vibronic peak and I_3 is the third vibronic peak of the pyrene.[101]

Theoretical *CMC* values were calculated using Clint,[119] formalism. Micellar structure and composition of micelle in the molecular level were calculated using different proposed models, *viz.,* Rubingh's, Rosen, Motomora and SPB. Rubingh's formalism has been successfully utilized to describe

and correlate the observed non-idealities in the micellization behavior in case of the different surfactants mixtures.[204] Different interaction parameters, *viz.*, mole fraction of surfactant at the micellar interface (X^{σ}), interaction parameters at the bulk/ interface (β^{R}/β^{σ}), activity coefficient (f) and ideality/non-ideality of the mixing processes of individual component were evaluated, calculated using Q-basic 64-data base (QB64) software programme. Q-basic is a short form of Quick Beginners. Symbolic instruction code is an integrated development environment (IDE) and interpreter for a variety of BASIC programming languages based on Quick BASIC software. The theoretical values of *CMC* were calculated by different physicochemical process and its comparison with the experimental values are subsequently discussed.[85] The average experimental *CMC* values are calculated by different physicochemical process and their comparison with theoretical *CMC* due to the associative interaction between $(C_{12}AAS)Na_2$ and HTAB being subsequently discussed.[203]

4. RESULTS AND DISCUSSION

4.1. Critical Micelle Concentration (CMC)

CMC of pure HTAB was found to be 0.72 mM,[203] while those of disodium salt of *N*-dodecyl aminomalonate ($C_{12}MalNa_2$), *N*-dodecyl aminoaspartate ($C_{12}AspNa_2$), and *N*-dodecyl aminoglutamate ($C_{12}GluNa_2$) were 51.2, 46.3 and 36.45 mM, respectively.[203] With increasing mole fraction of amino acid based surfactant $\alpha_{(C_{12}AAS)_2Na_2}$, *CMC* values gradually increased from the initial lower value of HTAB as shown in Figure 1, and also summarized in Table 1. Experimental *CMC* values are lower than the theoretically calculated *CMC* of different $(C_{12}AAS)Na_2$+HTAB mixtures.[205] Significant negative deviations from the theoretically calculated values are due to the associative interaction between the $(C_{12}AAS)Na_2$ and HTAB.[206] Competitive interfacial adsorption is observed due to the hydrophobic interaction between $(C_{12}AAS)Na_2$ and HTAB, assisted by charge neutralization in the micelle. Strong attractive interactions between the oppositely charged surfactants in the bulk solvent and interface can be explained using the theoretical models proposed by Clint,[94] Rosen,[97] Rubingh [90,120] and Sarmoria-

Puvvada-Blankschtein.[207] Composition of micelles in case of oppositely charged mixed surfactants are usually different from the interfacial and bulk compositions.[208] Synergistic interactions are reflected through the occurrence of substantially lower *CMC* in case of surfactant mixtures than the theoretically calculated values. The activity coeffficent of surfactant in the micelle (*f*), interaction parameter between the components of mixed surfactant (β^{R}), micellar mole fraction of (C_{12}AAS)Na_2 ($X_{Na_{2AAS}}$), micellar mole fraction of HTAB (X_{HTAB}), mole fraction of (C_{12}AAS)Na_2 at the interface (X_1^{σ}) and micellar mole fraction of (C_{12}AAS)Na_2 at the ideal state (X_1^{ideal}) values were also evaluated. Components 1 and 2 are the designations of binary components (C_{12}AAS)Na_2 and HTAB, respectively. The Clint model is known to provide reasonable information about the amphiphile mixture in solution. Variation of *CMC* with the surfactant mole fraction and the micellar composition of binary surfactants can furtherbe assessed using the Clint model as explained in the following section.

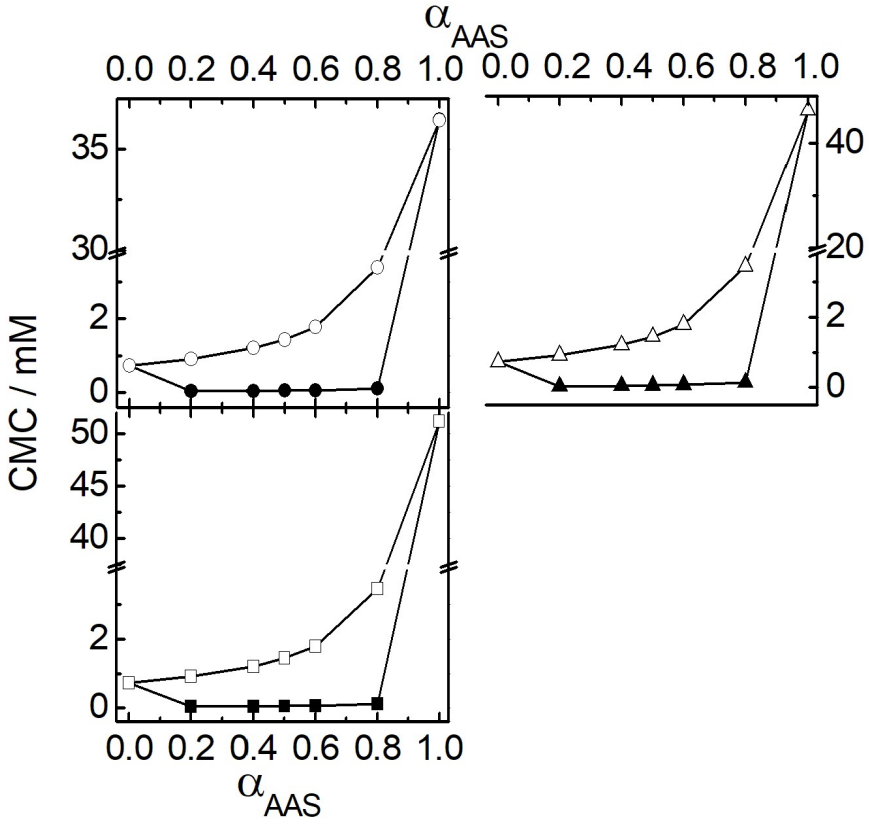

Figure 1. Variation of CMC with the mole fraction of (C_{12}AAS)Na_2, $\alpha_{(C_{12}AAS)_2Na_2}$ at 298 K. Systems: O, C_{12}MalNa$_2$-HTAB; Δ, C_{12}AspNa$_2$-HTAB and □, C_{12}GluNa$_2$-HTAB. Open symbols correspond to the theoretically calculated CMC values using Clint formalism and the closed symbols indicate experimentally observed average CMC values.

Table 1. Values of the Experimental *CMC* (average), Theoretical *CMC* (calculated), activity coefficient of $(C_{12}AAS)Na_2$ (f_1), HTAB (f_2), interaction parameter (β^R), micellar composition of X_{AAS} and X_{HTAB} calculated from Rubingh model, micellar mole fraction at the ideal state of the component (X_1^{ideal}) calculated by Motomura equation and interfacial parameters (β^σ) and micellar composition at the interface (X^σ) values calculated from Rosen model for $(C_{12}AAS)Na_2$-HTAB mixed surfactant systems at 298K.

$\alpha_{(C_{12}AAS)_2Na_2}$	*CMC*/mM		f_1	f_2	$X_{AAS}(X_1)$	$X_{HTAB}(X_2)$	(-) β^R	X_1^{ideal}	X_1^σ	(-) β^σ
	Experimental average	Theoretical								
HTAB-C_{12}MalNa$_2$										
1.0	51.20	-	-	-	-	-	-	-	-	-
0.8	0.151	3.38	0.0061	0.0702	0.426	0.574	14.48	0.069	0.439	15.44
0.6	0.092	1.78	0.0028	0.0768	0.404	0.596	15.72	0.027	0.418	16.73
0.5	0.073	1.43	0.0020	0.0794	0.395	0.605	16.42	0.018	0.410	17.48
0.4	0.062	1.18	0.0012	0.0849	0.391	0.609	17.43	0.012	0.405	18.49
0.2	0.043	0.88	0.0006	0.0884	0.372	0.628	19.17	0.005	0.388	20.30
0.0	0.730	-	-	-	-	-	-	-	-	-
HTAB-C_{12}AspNa$_2$										
1.0	46.30	-	-	-	-	-	-	-	-	-
0.8	0.143	3.43	0.0063	0.0602	0.409	0.591	15.84	0.056	0.435	16.37
0.6	0.081	1.79	0.0028	0.0668	0.388	0.612	16.57	0.022	0.416	17.54
0.5	0.062	1.44	0.0018	0.0714	0.381	0.619	16.91	0.014	0.409	17.92
0.4	0.054	1.20	0.0011	0.0719	0.377	0.623	18.05	0.009	0.403	19.07
0.2	0.042	0.89	0.0004	0.0759	0.364	0.636	18.91	0.004	0.383	20.02
HTAB-C_{12}GluNa$_2$										
1.0	36.45	-	-	-	-	-	-	-	-	-
0.8	0.117	3.46	0.0048	0.0583	0.422	0.578	15.96	0.047	0.425	16.83
0.6	0.061	1.80	0.0019	0.0586	0.403	0.597	17.47	0.018	0.404	18.39
0.5	0.051	1.46	0.0014	0.0609	0.395	0.605	17.94	0.012	0.398	18.92
0.4	0.042	1.21	0.0009	0.0703	0.389	0.611	18.66	0.008	0.393	19.65
0.2	0.041	0.91	0.0005	0.0752	0.368	0.632	19.10	0.003	0.380	20.19

4.2. Interaction between oppositely charged surfactants and theoretical propositions.

4.2.1. Clint model

Surfactants in the bulk solvent and at air-water interface, exhibit either ideal or non-ideal mixing behavior between the components. *CMC* value of mixed surfactants can also be theoretically calculated using Clint formalism assuming ideal mixing: [119]

$$\frac{1}{CMC_{\mathrm{cal}}} = \sum_{\mathrm{i}=1}^{n} \frac{\alpha_{\mathrm{i}}}{CMC_{\mathrm{i}}} \quad (1)$$

where, CMC_{i} is the *CMC* of neat surfactant '*i*' in solvent and '*n*' is the number of surfactants in the mixture. It is observed that the average experimental *CMC* values, which correspond to the average of the *CMC* values determined by surface tension, conductivity, UV-vis absorption/emission spectroscopy) of mixed surfactants at different mole fractions exhibit significant negative deviations from theoretically calculated *CMC* (CMC_{cal}), indicating associative interaction among the oppositely charged surfactants, as shown in Figure 1. A secondary cause of this trend for $(C_{12}AAS)Na_2$-HTAB mixtures is the enhanced hydrophobicity through the formation of pseudo-double tailed entities (formed by the cationic and anionic surfactants) and ion pairing of the surfactant head groups. [85] In case of *N*-dodecyl amino malonate, there is only one carbon atom in between two carboxylate groups. In case of aspartate and glutamate the numbers of carbon atoms between the two carboxylate moieties are two and three respectively. The sequential increase in the number of carbon atoms that act as speacer between the two carboxylate moieties favor micellization due to enhanced hydrophobicity. The progressive enhancement in the hydrophobicity, contributed by the methylene group between the two carboxylate groups, also favours negative deviation in the experimental *CMC* values.[209] It is expected that the structural difference between HTAB and $(C_{12}AAS)Na_2$ is the most important causative factor for the deviations of experimental and theoretical *CMC*s. With increasing hydrophobicity of the spacer, synergistic interaction between HTAB and the $(C_{12}AAS)Na_2$ also increases. Therefore, a hydrophobic interaction between the monomers of the

surfactant pair at the air-water interface likely follows the extent of deviation between theoretical and measured CMC: $C_{12}MalNa_2$+HTAB > $C_{12}AspNa_2$+HTAB > $C_{12}GluNa_2$+HTAB. The Clint model fails to properly explain (i) the deviation of experimental *CMC* from the CMC_{cal} (using Eq. 1) based on an ideal mixture, (ii) interaction among different surfactants in the aggregated state, (iii) the micellization behavior for concentrated solutions (systems with very high *CMC*), and (iv) the ability of mixed surfactants in forming the micelles that enhance the hydrophobic environment in comparison to the micelles formed by neat HTAB or (C_{12}AAS)Na_2. Rosen et al.[1] Modified Clint's model with the following propositions: (i) the mole fraction of a particular component in the micelle is lower than the mole fraction of the component in the overall solution, indicating a lower extent of transfer from solution to micelle, (ii) mixtures show synergism, and (iii) increasing hydrophobicity leads to increasing synergistic interaction.

4.2.2. Rosen model

The Rosen model can assess the magnitude of interaction between oppositely charged surfactants that form monomolecular films at air-water interface.[210] Using regular solution theory (RST), [120] and standard surface tension methods, [211] the composition of individual components in the mixed monolayer, mole fraction of (C_{12}AAS)Na_2 at the interface (X_1^σ) and interfacial interaction parameter (β^σ) can be evaluated. β^σ at air-water interface was proposed using the "successive method" (method of iteration, as described below), [169,170] assuming the formation of monolayer at the air-water interface. For this purpose, a computer program was made to estimate β^σ and micellar mole fraction of (C_{12}AAS)Na_2 in the air-water interface X_1^σ via the following equations:[169, 170]

$$\frac{(X_1^\sigma)^2 ln\,(X_1 C_{av}/X_1^\sigma C_1)}{(1-X_1^\sigma)^2 ln\,[1-X_1)\,C_{av}/(1-X_1^\sigma)C_2]} = 1 \quad (2)$$

$$\beta^\sigma = \frac{ln\,(X_1 C_{av}/X_1^\sigma C_1)}{(1-X_1^\sigma)^2} \quad (3)$$

β^{σ} *vs.* $\alpha_{(C_{12}AAS)_2Na_2}$ profiles are shown in Figure 2 (panel B). With increasing $\alpha_{(C_{12}AAS)_2Na_2}$, the magnitude of β^{σ} gradually decreases for each $(C_{12}AAS)Na_2$. The synergistic interaction (β^{σ}) between $(C_{12}AAS)Na_2$ and HTAB at air-water interface follow the sequence $C_{12}MalNa_2$+HTAB > $C_{12}AspNa_2$+HTAB > $C_{12}GluNa_2$+HTAB.

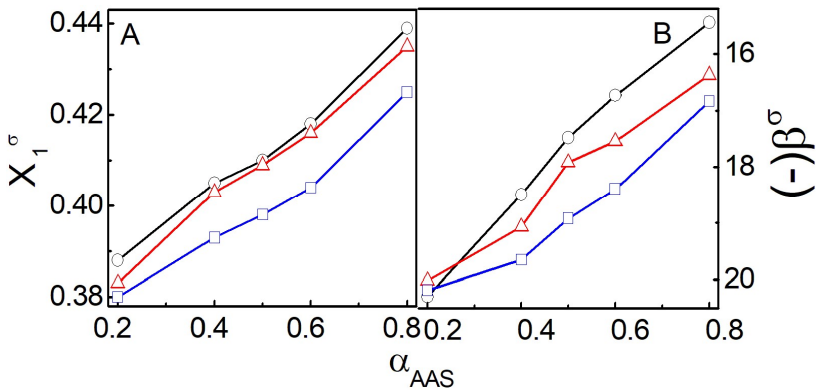

Figure 2. Variation of mole fractions of $(C_{12}AAS)Na_2$ at the interfacial monolayers (X_1^{σ}) synergistic molecular interaction (β^{σ}) calculated from Rosen model with the mole fraction of $\alpha_{(C_{12}AAS)_2Na_2}$ at 298K. Systems: O, $C_{12}MalNa_2$- HTAB; Δ, $C_{12}AspNa_2$-HTAB and □, $C_{12}GluNa_2$-HTAB.

Increasing the number of methylene groups between the carboxylates sterically favours its interaction with HTAB. The increased electrophilic interaction between the two oppositely charged head groups, inducing formation of mixed micelles, can explain the above sequence of β^{σ}.[212-216] On the other hand, the close proximity of the two carboxylate groups of $(C_{12}AAS)Na_2$ enhances electrostatic repulsion. X_1^{σ} *vs.* $\alpha_{(C_{12}AAS)_2Na_2}$ profiles are shown in Figure 2 (panel A). Unlike β^{σ}, X_1^{σ} gradually increases with increasing $\alpha_{(C_{12}AAS)_2Na_2}$, which suggest that HTAB interacts less favorably with $(C_{12}AAS)Na_2$ at the air-water interface to form mixed monolayer. With increasing $\alpha_{(C_{12}AAS)_2Na_2}$, X_2 and $(1\text{-}X_1^{\sigma})$ values gradually decreased, which indicates that the mixed micelles contain a larger proportion of HTAB compared to the overall solution, as a result of a smaller cross sectional area and higher hydrophobicity for HTAB.[85] For all compositions, X_2^{σ} follows the order: $C_{12}MalNa_2$ < $C_{12}AspNa_2$ < $C_{12}GluNa_2$. The trend can be explained by $C_{12}MalNa_2$ being less bulky and hydrophilic than the other two Na_2AAS due to the absence of methylene group between two carboxylate anions, thereby enabling $C_{12}MalNa_2$ to more strongly interact

with HTAB and remain associated with the micellar surface.[217] The same trend is also reflected by lower aggregation number of $C_{12}MalNa_2$ compared to $C_{12}AspNa_2$ and $C_{12}GluNa_2$, (Figure 3).[205]

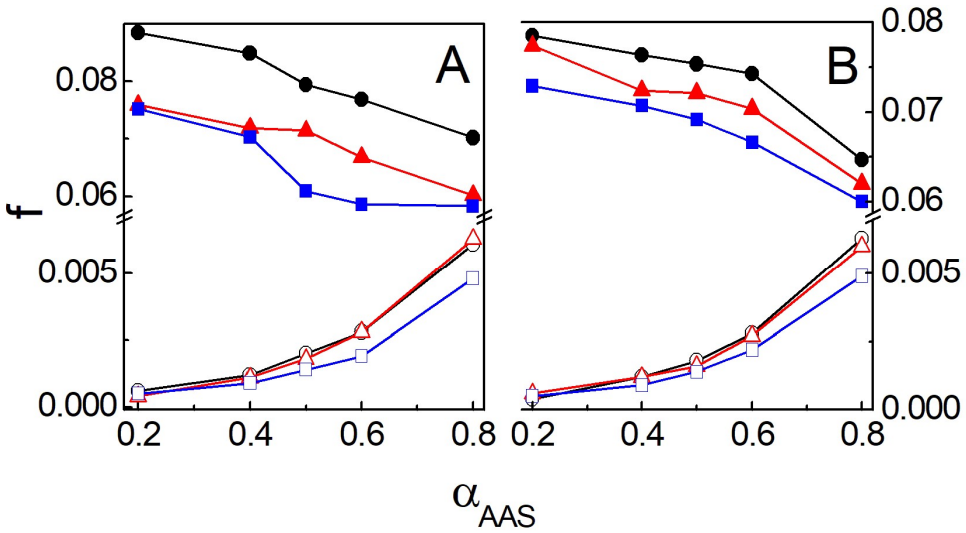

Figure 3. Variation of activity coefficient of $(C_{12}AAS)Na_2$ (f_1), HTAB (f_2) calculated from Rubingh (panel A) and SPB (panel B) model. Systems: O, $C_{12}MalNa_2$-HTAB; Δ, $C_{12}AspNa_2$-HTAB and □, $C_{12}GluNa_2$-HTAB. Open symbols correspond to the activity coefficient of $(C_{12}AAS)Na_2$ and the closed symbols indicate activity coefficient of HTAB.

The stronger interaction between $C_{12}MalNa_2$ and HTAB are also reflected by lower β^{σ} values (Table 1).[212-216] Negative β^{σ} values for all the $(C_{12}AAS)Na_2$+HTAB mixed micelles also indicate mutual interaction between the monomers of surfactant pair at air-water interface.[97] The values of X_1^{σ} for all the three binary surfactant mixtures are smaller than $X_1(X_{Na_{2AAS}})$, indicating that $(C_{12}AAS)Na_2$ are less prominent at the air-liquid interface than HTAB.

4.2.3. Rubingh model

Clint's proposition about the stronger deviation of experimental *CMC* with respect to theoretical *CMC* was also addressed by Rubingh. Rubingh's model for ideal/non-ideal mixed systems is based on regular solution theory (RST). Thus following modification of the equation 1 was made according to the proposition of Rubingh:[120]

$$\frac{1}{CMC} = \sum_{i=1}^{n} \frac{\alpha_i}{f_i CMC_i} \qquad (4)$$

where, f_i is the activity coefficient of i^{th} component in a micelle. Molecular interaction parameters were studied in the light of RST.[120] Unlike the models described above, RST is capable to predict the synergistic as well as antagonistic interaction between the surfactant mixtures. The f_1 and f_2 *vs.* $\alpha_{(C_{12}AAS)_2Na_2}$ profiles are shown in Figure 4 (panels A and B, respectively).

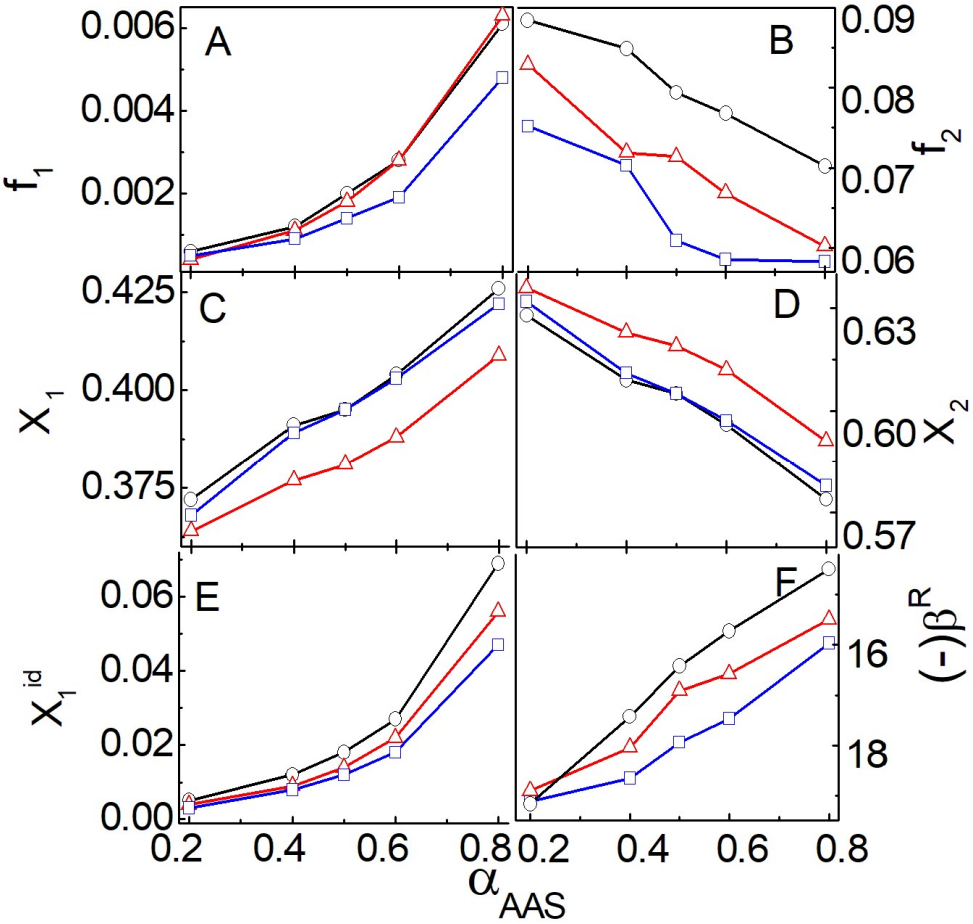

Figure 4. Variation of activity coefficient of $(C_{12}AAS)Na_2$ (f_1), activity coefficient of HTAB (f_2), micellar composition of $(C_{12}AAS)Na_2$ (X_{AAS}) and micellar composition of HTAB (X_{HTAB}) values, calculated using Rubingh model, micellar mole fraction of the ideal state (X_1^{ideal}) and interaction parameter (β^R) values, calculated using Motomura equation with the mole fraction of $\alpha_{(C_{12}AAS)_2Na_2}$ at 298K. Systems: O, $C_{12}MalNa_2$-HTAB; Δ, $C_{12}AspNa_2$-HTAB and □, $C_{12}GluNa_2$-HTAB.

With increasing $\alpha_{(C_{12}AAS)_2Na_2}$, f_1 values increase while the f_2 values decrease. Extent of increase in f_1 values are less than the decrease in f_2 values for all the combinations. The decrease of f_2 values follow the order $C_{12}MalNa_2$+HTAB > $C_{12}AspNa_2$+HTAB > $C_{12}GluNa_2$+HTAB. *CMC* values for the mixtures are similar to the CMC of pure HTAB, indicating that HTAB plays fundamental role for the synergism. Higher values of f_2 (HTAB) than f_1 $(C_{12}AAS)Na_2$) indicate the significant contribution of HTAB due to its

larger head group size (Figure 3). Using RST, Rubingh proposed Eqs. 4-7 for determining different parameters of micellization of binary surfactants:[2, 120]

$$\beta^{\mathrm{R}} = \left(ln \frac{\left[\frac{(CMC_{\mathrm{av}}\alpha_1)}{(CMC_1(1-X_2))}\right]}{{X_2}^2} \right) \tag{5}$$

where, β^{R} is the interaction parameter between the components in the micelle. Micellar mole fraction of (C_{12}AAS)Na_2 (X_{AAS}) and HTAB (X_{HTAB}) *vs.* $\alpha_{(C_{12}AAS)_2Na_2}$ profiles are shown in Figure 4 (panels C and panel D, respectively). Relative proportions of (C_{12}AAS)Na_2 in the micelles gradually increase with increasing $\alpha_{(C_{12}AAS)_2Na_2}$. Non-ideality in the mixing behavior was further rationalized by Rubingh using Eq. 6 as:[120]

$$\frac{(1-X_2)^2 \ln\left[\frac{CMC_{\mathrm{av}}\alpha_1}{CMC_1(1-X_2)^2}\right]}{(X_2)^2 \ln\left[\frac{CMC_{\mathrm{av}}\alpha_{12}}{(CMC_2(X_2)}\right]} = 1 \tag{6}$$

Eq. 6 was employed to solve for X_2 iteratively using a computer program. After obtaining X_2 from Eq. 6, β^{R} is calculated from Eq. 5 Subsequently, f_1 and f_2 are calculated using Eq. 7: [2, 120]

$$f_{\mathrm{i}} = \exp\left[\beta^R(1 - X_i^2)\right] \tag{7}$$

f =1 indicates ideal mixed surfactant systems. The micellar mole fractions obtained from the Rubingh model have been compared with the micellar mole fraction of (C_{12}AAS)Na_2 at the ideal state (X_1^{ideal}), with the help of Motomura's approximation:[218]

$$X_1^{\mathrm{ideal}} = \frac{\alpha_1 CMC_2}{\alpha_1 CMC_2 + \alpha_2 CMC_1} \tag{8}$$

X_1^{ideal} *vs.* $\alpha_{(C_{12}AAS)_2Na_2}$ profiles are shown in Figure 4 (panel E). All of the parameters calculated from Eqs. 5-8 are summarized in Table 1. With increasing $\alpha_{(C_{12}AAS)_2Na_2}$, X_1^{ideal} gradually increases for all three (C_{12}AAS)Na_2. X_1^{ideal} values follow the order $C_{12}MalNa_2$ > $C_{12}AspNa_2$ > $C_{12}GluNa_2$. It is observed from Table 1 that micellar composition of HTAB in the ideal state (X_2^{ideal}), calculated by Motomura's

approximation show the greater values than those calculated for RST. [219] β^R values for all three systems investigated are negative, indicating strong attractive interaction between (C_{12}AAS)Na_2 and HTAB. [212-216] With increasing $\alpha_{(C_{12}AAS)_2Na_2}$, the magnitude of β^R values gradually decreases (Figure 4, panel F). X_1^{ideal} for C_{12}MalNa_2, C_{12}AspNa_2 and C_{12}GluNa_2 differ significantly from X_{AAS} values, calculated by RST. Hence, the micellization of the (C_{12}AAS)Na_2-HTAB systems is non-ideal in nature from the view point of Motomura approximation. β^R values for (C_{12}AAS)Na_2-HTAB systems are found to be composition dependent, in contrast with RST, which assumes β^R should remain independent of composition. The composition dependency of β^R has also been reported in literature for several surfactant mixtures, manifesting the shortcoming of the Rubingh's approach for binary surfactant mixtures.[220, 221]

4.2.4. Sarmoria-Puvvada-Blankschtein (SPB) model

Motomura et al. (1984) proposed the 'SPB' model that estimates the phase separation based on molecular thermodynamics theory, where optimal micellar composition was quantified by Sarmoria-Puvvada-Blankschtein for binary surfactant mixtures.[207] The Clint equation,[119] can be rewritten in the following form:

$$\frac{1}{CMC_{cal}} = \frac{\alpha_1}{f_1 CMC_1} + \frac{\alpha_2}{f_2 CMC_2} \quad (9)$$

Activity coefficients (f_i, where $f_i \neq 1$) are calculated by the following equations: [207]

$$f_1 = exp\,[\beta_{12} \frac{(1-\alpha^*)^2}{kT}] \quad (10)$$

$$f_2 = exp\,[\beta_{12} \frac{(\alpha^*)^2}{kT}] \quad (11)$$

where, β_{12} is the specific interaction between (C_{12}AAS)Na_2 and HTAB (analogas to the β^R) and α^* is the predicted optimal micellar composition, designated by X_{SPB} (the composition at which the free energy of mixed micellization attains its minimum value),[207] k is the Boltzman constant and T is the temperature in absolute scale. Results are summarized in Table 2 and Figure 5.

Table 2. Values of the activity coefficient of $(C_{12}AAS)Na_2$ (f_1), HTAB (f_2), *CMC* values calculated by SPB model, (X_{SPB}), theoretically calculated *CMC* and interaction parameter (β^R, KT) of $(C_{12}AAS)Na_2$-HTAB mixed surfactant systems at different mole fraction of $(C_{12}AAS)Na_2$ at 298 K.

$\alpha_{(C_{12}AAS)_2Na_2}$	f_1	f_2	X_{SPB}	$(-)\beta^R$ (KT)
HTAB-C_{12}MalNa$_2$				
0.8	0.0063	0.06467	0.426	14.51
0.6	0.0028	0.07427	0.404	15.62
0.5	0.0018	0.07535	0.400	16.43
0.4	0.0012	0.07636	0.391	17.32
0.2	0.0004	0.07850	0.372	18.92
HTAB-C_{12}AspNa$_2$				
0.8	0.0060	0.06000	0.421	15.51
0.6	0.0027	0.07111	0.400	16.62
0.5	0.0016	0.07212	0.394	17.88
0.4	0.0012	0.07238	0.388	18.09
0.2	0.0006	0.07740	0.367	19.20
HTAB-C_{12}GluNa$_2$				
0.8	0.0049	0.06000	0.409	15.86
0.6	0.0022	0.06660	0.387	17.00
0.5	0.0014	0.06917	0.381	17.83
0.4	0.0009	0.07069	0.376	18.58
0.2	0.0005	0.07290	0.364	18.99

With increasing $\alpha_{(C_{12}AAS)_2Na_2}$, f_1 gradually increases, (Figure 5, panels A and B). The X_{SPB} values for all the combinations vary almost linearly with $\alpha_{(C_{12}AAS)_2Na_2}$(Figure 5, panel C). β^R *vs.* $\alpha_{(C_{12}AAS)_2Na_2}$profiles are shown in Figure 5 (panel D).

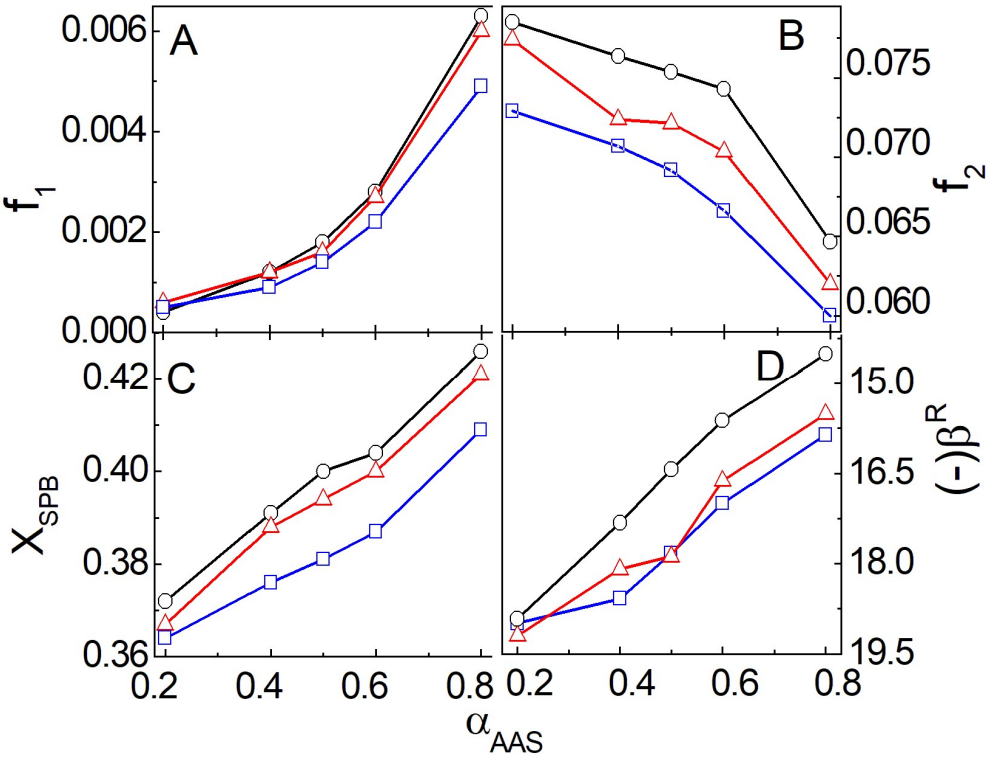

Figure 5. Variation of activity coefficient of $(C_{12}AAS)Na_2$ (f_1), activity coefficient of HTAB (f_2), CMC values calculated by SPB model, (X_{SPB}) and interaction parameter (β^R) values were calculated by SPB model with the mole fraction of $\alpha_{(C_{12}AAS)_2Na_2}$ at 298K. Systems: O, $C_{12}MalNa_2$- HTAB; Δ, $C_{12}AspNa_2$-HTAB and □, $C_{12}GluNa_2$-HTAB.

Negative lower β^R values demonstrate stronger synergistic interaction between $(C_{12}AAS)Na_2$ and HTAB. [220, 221] β_{12} and α^* values were calculated using trial and error method by means of iteration using the following equation, [207] by minimizing the standard deviation between the equation's left- and right-hand side:

$$\frac{\beta_{12}(1-2\alpha^*)}{kT} + ln\frac{\alpha^*}{(1-\alpha^*)} = ln\frac{\alpha_1 CMC_2}{\alpha_2 CMC_1} \quad (12)$$

By the substitution of α^* (X_{SPB}) into Eqs. 11 and 12, β_{12} and f were calculated. From Tables 1 and 2 it is evident that X_{SPB} of various AAS components are comparable with X_{Mal}, X_{Asp} and X_{Glu} calculated using the RST model. Calculated f, β_{12} and X for the three different systems are nearly the same between the Rubingh's and SPB models.

4.2.5. Thermodynamics of micellization

From the RST model,[120] different thermodynamic parameters can be derived,[222] assuming that the excess entropy of mixing is zero, as has been performed for other surfactant mixtures.[170, 223-226] Gibbs excess free energy (G^{Ex}), excess enthalpy (H^{Ex}) and enthalpy of micellization (ΔH_m) can be calculated using Eq.13: [223, 224]

$$G^{Ex} = H^{Ex} = \Delta H_m = \mathrm{RT}\,[X_1 \ln(f_1) + X_2 \ln(f_2)] \quad (13)$$

X_1, X_2, f_1 and f_2 values were calculated from Rubingh's model (Table 1). [120]

Table 3. Values of the thermodynamical parameters for the determination of excess free energy of micellization (G^{Ex}), enthalpy of micellization (ΔH_m), excess enthalpy (H^{Ex}), free energy of micellization for ideal (ΔG_m^{ideal}) / non ideal (ΔG_m) mixing and entropy of micellization (ΔS_m) for non ideal mixing derived from RST of $(C_{12}AAS)Na_2$ - HTAB mixed surfactant systems at different stiochiometric mole fraction of $(C_{12}AAS)Na_2$ at 298 K.

$\alpha_{(C_{12}AAS)_2Na_2}$	(-) $G^{Ex} = \Delta H_m = H^{Ex}$ kJ. mol^{-1}	(-)ΔG_m^{ideal} kJ. mol^{-1}	$(-)\Delta G_m$ kJ. mol^{-1}	ΔS_m J.K^{-1}. mol^{-1}	$\lvert T\Delta S_m / \Delta G_m \rvert$
HTAB-C_{12}MalNa$_2$					
0.8	9.14	1.69	10.8	5.67	0.16
0.6	9.67	1.67	11.3	5.61	0.15
0.5	9.88	1.66	11.5	5.58	0.14
0.4	10.2	1.66	11.8	5.56	0.14
0.2	10.6	1.63	12.2	5.48	0.13
HTAB-C_{12}AspNa$_2$					
0.8	9.25	1.68	10.9	5.62	0.15
0.6	9.75	1.65	11.4	5.55	0.14
0.5	10.0	1.65	11.7	5.52	0.14
0.4	10.4	1.64	12.1	5.51	0.14
0.2	11.1	1.62	12.7	5.45	0.13
HTAB-C_{12}GluNa$_2$					
0.8	9.65	1.69	11.3	5.66	0.15
0.6	10.4	1.67	12.1	5.60	0.14
0.5	10.6	1.66	12.3	5.58	0.14
0.4	10.8	1.65	12.4	5.56	0.13
0.2	10.9	1.63	12.6	5.47	0.13

Gibbs free energy of micellization for ideal mixing ΔG_m^{ideal} can be calculated by the following equation: [223, 224]

$$\Delta G_m^{ideal} = RT[X_1 \, ln \, (X_1) + X_2 \, ln \, (X_2)] \quad (14)$$

Gibbs excess free energy ($G^{Ex} = \Delta G_m - \Delta G_m^{ideal}$) indicates the deviation from the ideality for the mixing. ΔG_m designates the non-ideal free energy of micellization, given by Eq.15:

$$\Delta G_m = RT[X_1 \, ln \, (X_1 f_1) + X_2 \, ln \, (X_2 f_2)] \quad (15)$$

Changes in entropy of micellization (ΔS_m) can be obtained from Eq.16:

$$\Delta S_m = \frac{\Delta H_m - \Delta G_m}{T} \quad (16)$$

The values of all the parameters discussed above, are presented in Figure 6 and Table 3. It is evident that with increasing mole fraction of HTAB, ΔH_m increases (Figure 6, panel A).

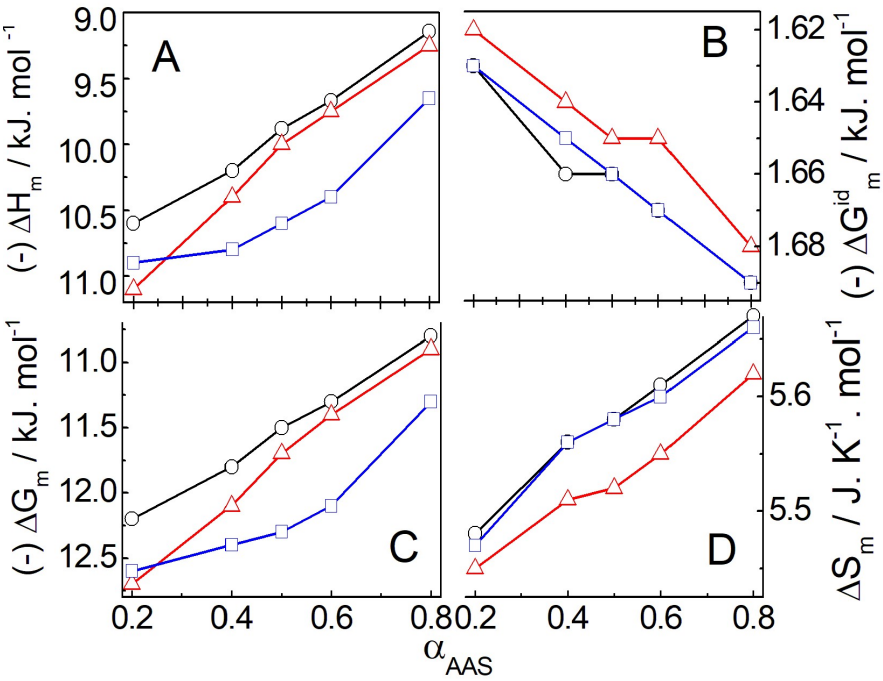

Figure 6. Variation of excess free energy of micellization (G^{Ex}), enthalpy of micellization (ΔH_m), excess enthalpy (H^{Ex}) of ($C_{12}AAS$)Na_2 ($G^{Ex} = \Delta H_m = H^{Ex}$), free energy of micellization for ideal mixing (ΔG_m^{ideal}), non ideal mixing (ΔG_m) and entropy of micellization (ΔS_m) for non ideal mixing (β^R) values, calculated by using Rubingh model with the mole fraction of $\alpha_{(C_{12}AAS)_2Na_2}$ at 298K. Systems: O, C_{12}MalNa$_2$- HTAB; Δ, C_{12}AspNa$_2$-HTAB and □, C_{12}GluNa$_2$-HTAB.

When comparing the three (C_{12}AAS)Na_2, it is observed that the ΔH_m values follow the sequence $C_{12}MalNa_2$+HTAB > $C_{12}AspNa_2$+HTAB > $C_{12}GluNa_2$+HTAB. There are two opposing factors that contribute to ΔH_m: (i) the energy released due to the loss of translational energy of surfactant monomers as a result of electrostatic and hydrophobic interaction for the micellization, and (ii) energy required to break the organized structure of bulk water. As the mole fraction of HTAB is increased, hydrophobic interactions increase, leading to a more exothermic process of micellization. For the same reason, ΔH_m values increase with the sequential increase in the methylene group of the spacer when comparing $C_{12}MalNa_2$ to $C_{12}AspNa_2$ to $C_{12}GluNa_2$. The ΔG_m values are found to be more negative than the ΔG_m^{ideal}, which indicates the spontaneity of micellization (Figure 6, panel B). The negative value of G^{Ex} further supports the occurrence of synergistic interactions.[223] The same trends are observed for ΔH_m and ΔG_m (Table 3). Variation of ΔG_m for the mixed micelles of HTAB and (C_{12}AAS)Na_2 with $\alpha_{(C_{12}AAS)_2Na_2}$ are presented in the panel C of Figure 6. The entropic contribution of $T\Delta S_m$ towards ΔG_m is found to be 13-16%, which indicates that the entropic contribution (ΔS_m) to the mixed micellization is less than the enthalpic contribution (ΔH_m). With increasing $\alpha_{(C_{12}AAS)_2Na_2}$, ΔS_m values gradually increase, (Figure 6, panel D), indicating spontaneous micellization and interfacial adsorption. Furthermore, the degree of disorderness increases due to micellization and the entropy change, favorable for the formation of mixed micelles, as demonstrated by the positive ΔS_m values. [223, 224]

5. Conclusions

This theoretical investigation has simplified the molecular thermodynamics-related theory for micelle formation by mixed surfactants systems. Different working models to predict *CMC* of non-ideal binary surfactants as well as specific interactions were compared. The models provided reasonable quantitative predictions of the different micellization parameters for cationic-anionic mixed surfactant systems. The simplified "working models" employed herein can act as valuable preliminary screening tools in the design and selection of non-ideal surfactant mixtures for practical applications. Synergistic

interaction behavior of (C_{12}AAS)Na_2-HTAB mixtures were assessed using Rubingh's, Rosen, Motomura and SPB models. The experimental *CMC* values are lower than the predicted values calculated from Clint formalism, indicating non-ideality in the mixing behavior. *CMC* values gradually increase with the increasing proportion of Na_2AAS. Oppositely charged surfactants can localize in vicinity to each other and interact mainly at the micellar surface. The two carboxylate groups of (C_{12}AAS)Na_2 repel each other, the extent of which is minimized by HTAB through electrostatic attraction; thus the micellar size gradually decreases with increasing $\alpha_{(C_{12}AAS)_2Na_2}$. A maximum number of HTAB molecules become available on the micellar surface, leading to the formation of closed packed micellar structures.[203] The binary mixtures show significant synergism (negative β^R value).[220,221] With increasing hydrophobicity of the spacer, synergistic interactions between the surfactant components also increase. With increasing $\alpha_{Na_{2AAS}}$, the magnitude of β^R decreases,[212-216], X_1^{ideal}, X_1 (Rubingh model) and X_1^{σ} (Rosen model) gradually increase with an increase of $\alpha_{(C_{12}AAS)_2Na_2}$. The magnitude of β^{σ} at air-water interface gradually decreases with increasing $\alpha_{(C_{12}AAS)_2Na_2}$ and follows the order $C_{12}MalNa_2$+HTAB > $C_{12}AspNa_2$+HTAB > $C_{12}GluNa_2$+HTAB. ΔG_m values are more negative than ΔG_m^{ideal}, which indicate that the micellization process is spontaneous. Mixed micellization of HTAB-(C_{12}AAS)Na_2 is enthalpy driven where ΔH_m values decrease with increasing $\alpha_{(C_{12}AAS)_2Na_2}$.[223, 224] It is believed that theoretical investigations of mixed micelles of such binary surfactants can provide new insights, which will eventually help in understanding the bulk and interfacial activities of mixed surfactant systems. Strong synergistic interaction between the oppositely charged surfactants can result in the formation of liquid crystal, viscous gels and even vesicles. However, further theoretical investigations employing molecular dynamics could support the propositions made here, in the future. Oppositely charged mixed surfactants form different types of aggregates as stated earlier; so the knowledge on the surface morphology by phase contrast, polarization optical microscopy (POM), fluorescence microscopy (FM), field emission scanning electron microscopy (FE-SEM) and small angle X-ray scattering (SAXS) studies are considered to be essential, being considered to be carried out in future.